Effect of Surplus Standing Liquid on Heat Transfer Resistance in the Heat Pipe (With Mesh Wick in a Horizontal Mode)

By

Makoto KAMATA* and Yoshio IKEDA*

(January 27, 1986)

Summary: It is an engineering practice to fill a heat pipe with working fluid of a quantity a little larger than the clearance volume of the screen wick as the most desirable volume of working fluid is unknown. However, it is foresseeable that excessive volume of working fluid deteriorates the performance of the heat pipe. This paper discusses a new method of computation for heat flow and temperature distribution in a heat pipe with the assumptions that the depth of working fluid in the heat pipe can be calculated from the pressure losses in the evaporation and condensation zones, that surplus fluid adheres to the inner wall of the screen wick forming a cylindrical layer of liquid, and that the heat transfer resistance of the container, screen wick and cylindrical layer of working fluid are connected in series. To validate the computation, experiments were performed and good agreement was obtained.

§I. INTRODUCTION

In Figure 1, the heat transfer circuit of a heat pipe is drawn, just like an electric circuit, with the paths of heat flow and the heat resistors. In this heat transfer circuit, the heat resistors, R3 and R7, representing the screen wick soaked with working fluid, have the most significant effect on the performance of the heat pipe. However, since the thermal conductivity of working fluid is small and the quantity of working flud contained in a heat pipe usually surpasses the clearance volume of the screen wick, the effect of surplus working fluid on the heat transfer performance of the heat pipe should be carefully examined. To investigate such effect, the top half of a screen wick was cut off and the state of surplus working fluid was observed. Based on this observation, the assumptions that surplus working fluid adheres only to the bottom of the heat pipe and that its depth varies step-wise through the evaporation zone, the adiabatic zone and the condensation zone were made. With these assumptions, heat flow through the heat pipe was calculated. Furthermore, with the other assumption that surplus working fluid adheres uniformly to the inner surface of the screen wick but the depth distribution in the axial direction varies step-wise through the evaporating zone, the adiabatic zone and the condensation zone, calculation were also made. The culculation with the second assumption gave better agreement with the experiments.

§II. EXPERIMENTAL MODEL

The experimental model, as shown in Figure 2, consists of a glass container which length, outer diameter and inne diameter are 500 mm, 20 mm, and 16 mm, respectively,

* Nippon Institute of Technology.

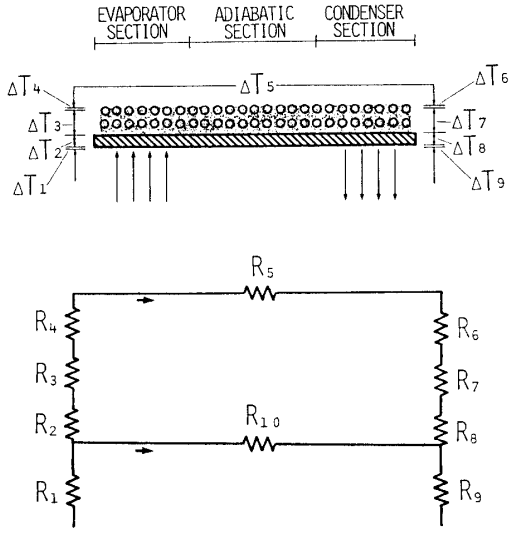

Fig. 1. Temperature drops and equivalent thermal resistance in a heat pipes.

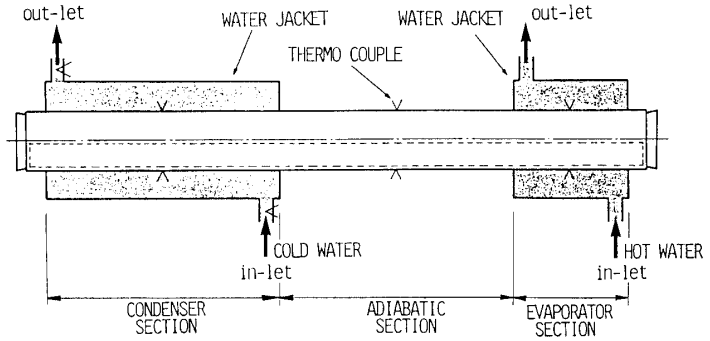

Fig. 2. Skematic illastration of the experimental apparatus.

and a screen wick made of two layers of 150-mesh bronze net. To install the screen wick inside the container, a coil spring is used. The water jackets for heating the evaporation zone and cooling the condensation zone are made of transparent acrylic acid resin to make it easier to observe the inside o the heat pipe. The lengths of these water jackets are 100 mm and 20 mm, respectively. As the working fluid, 9 cc of ethanol, accounting for approximately three times the volume of the screen wick, is enclosed in the container. The operating temperature was 40°C at the adiabatic zone. The heat flow was calculated from the temperature and volume of cooling water. However, since the water jackets were not insulated to provide see-through area, accuracy of the calculated heat flow was not very good.

§III. Results Of Observation

Figures 3 and 4 illustrate the state of working fluid as observed from side and top, respectively. White area represents the dry zone, gray area the wet wick, and the hatched area the stagnant liquid. (C) represents the state under 20 watt of heat flow where all area is wet and working fluid stagnate in the depth of 1–2 mm through the

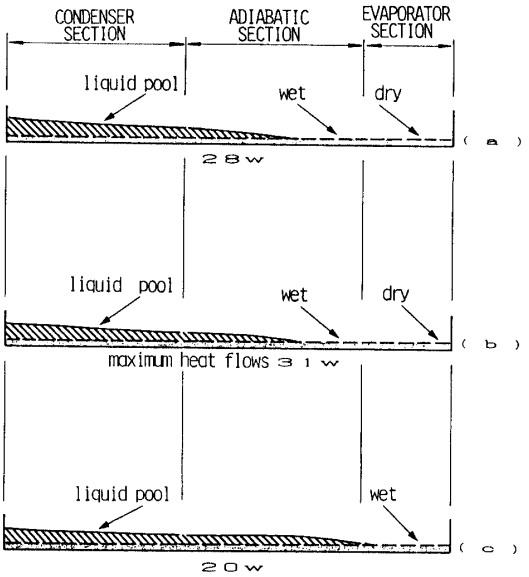

Fig. 3. Observation Results of liquid layer (side view)

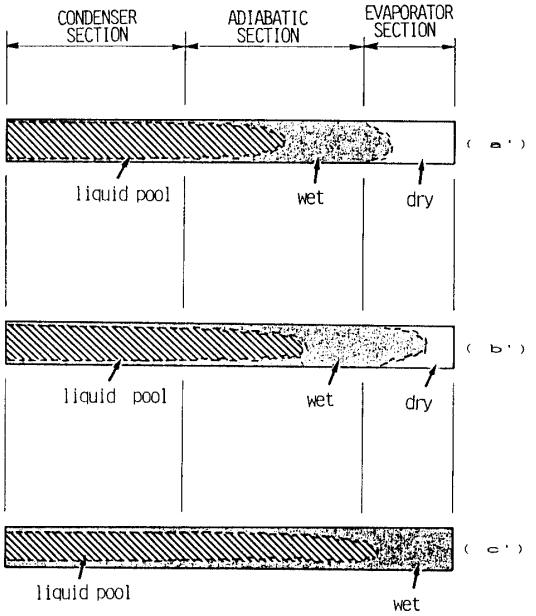

Fig. 4. Observation Results of liquid layer (plan view).

adiabatic zone and the condensation zone.

(B) represents the state under 31 watt of heat flow where a portion of the evaporation zone is dried up. In this state, the stagnant fluid layer looks thicker and heat flow seems to reach maximum. (A) represents the state under more heat flow where almost all area of the evaporation zone is dried up.

In this state heat flow turned out to be 28 watt. From these illustrations, it is observed that, as heat flow increases, surplus working fluid move towards the condensation zone and the depth becomes more than 1 mm.

Under a specific operating temperature, vapor pressure becomes saturated thereby the

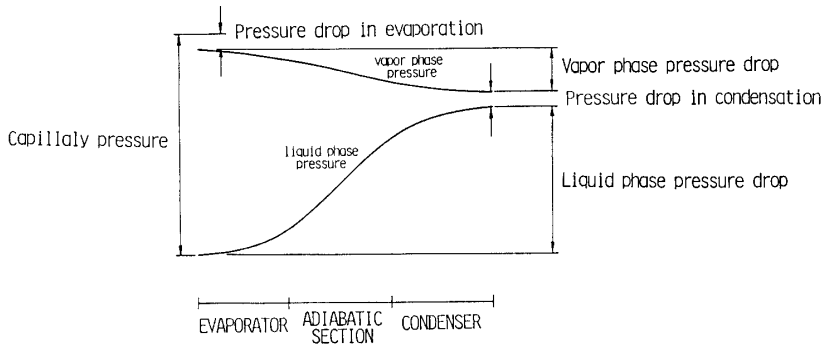

Fig. 5. Pressure drop distribution in heat pipes.

Pressure drop in the vapor

$$\Delta P_v = \frac{8 \mu_v Q L_{eff}}{\pi \rho_v r_v^4 \lambda} \qquad \text{----------(1)}$$

μ_v : Dynamic viscosity of vapor [N•sec/m^2]
ρ_v : Density of vapor [kg/m^3]
r_v : Radius of vapor space [m]
λ : Latent heat of vaporization [J/kg]

Pressure drop in vapor-liquid surface at evaporation

$$\Delta P_e = \frac{\sqrt{R T_{ve}}}{\sqrt{2\pi}} \frac{Q}{\alpha_c \{ \lambda - (1/2) R T_{ve} \} r_v L_e} \qquad \text{-------(2)}$$

Pressure drop in vapor-liquid surface at condensation

$$\Delta P_c = \frac{\sqrt{R T_{vc}}}{\sqrt{2\pi}} \frac{Q}{\alpha_c \{ \lambda - (1/2) R T_{vc} \} r_v L_c} \qquad \text{-------(3)}$$

R : Gas constant [J/kg•K]
α_c : Coefficient of evaporation or condensation [-]
T : Absolute temperature [K]
Q : Quantity of heat [W]]
λ : Latent heat of vaporization [J/kg]
r_v : Radius of vapor space [m]
L_e : Length of evaporator section [m]
L_c : Length of condenser section [m]

volume of liquid phase becomes constant regardless of the amount of heat flow. Therefore, the volumes of liquid phase in Figure 3 and 4 must be the same in spite of different amount of heat transportation. It is observed that working fluid tends to move towards the condensation zone as more heat flows. To account for this phenomenon, vapor flow and pressure loss due to evaporation and condensation are examined. By deviding the value of pressure loss in each phase by the value of specific weight of working fluid at its operating temperature, the pressure heads due to vapor flow, evaporation, and condensation can be obtained. A calculation made with 31 watt of heat flow yielded a value of 0.025 mm for the vapor flow pressure loss which is too small to compare with the observed value. However, the calculation of pressure losses due to evaporation and condensation demonstarated to yield values close to the observed values which are in the order of milimeter. In these calculation, the following equations (1), (2), (3) presented in the literature (1) were used.

The same literature (1) presents the pressure distribution inside the heat pipe such as shown in Figure 5. Ignoring the pressure loss due to fluid flow in the wick and the pressure loss due to vapor flow, a step-wide pressure distribution can be obtained. To balance this step-wise pressure distribution the surplus working fluid swells on the condensation zone.

Based on the above consideration, an assumption on the shape of swelled surplus working fluid is proposed as described in the following.

§IV. Proposed Model For The Shape Of Surplus Working Fluid

It is proposed to assume that working fluid of a depth providing necessary quantity of working fluid for circulation exists in the evaporation zone, that, in the adiabatic zone, surplus fluid stagnates arch-wise in the bottom of the heat pipe the depth being larger than the depth in the evaporation zone by an amount that accounts for the loss head due to evaporation, and that, in the condensation zone, the depth of the stagnant fluid becomes larger than the depth in the adiabatic zone by an amount that accounts for the loss head due to condensation. In this line, given the operating temperature and heat flow, the volume of liquid phase in each zone can be calculated. The total of these quantities accounts for the necessary quantity of working fluid for a given heat flow. If the quantity of enclosed fluid surpasses this necessary quantity, the depth of working fluid in the evaporation zone becomes thicker while the area of the arch-wise pond of working fluid in both adiabatic and condensation zones increases but the difference in the depth between adjacent zones are kept constant. The heat resistance increase subsequently.

In the above analysis the depth of fluid layer necessary for circulation was calculated by using Darcy's equation (4) with the following equation for the permeability of screen wick (5) including inter-layer clearance, β and number of layers, n.

§V. Heat Transfer Resistance Of Heat Pipe

The heat transfer resistance of surplus working fluid was calculated with either of the following two assumptions:

(a) The heat pipe can be devided into two parts, one including the whole surplus fluid standing arch-wise in the bottom of the heat pipe and the other including the rest of the heat pipe to which no standing fluid adheres.

ΔP_l : Pressure drop in liquid phase

$$\Delta P_l = \frac{\mu_l Q L_{eff}}{K_p A_w \rho_l \lambda} \qquad (4)$$

μ_l : Dynamic viscosity of liquid [N•sec/m²]
ρ_l : Density of liquid [kg/m³]
λ_l : Latent heat of vaporization [J/kg]
A_w : Wick cross sectional aria [m²]
L_{eff} : Effective length [m]
Q : Quantity of heat [W]

$$K_p = \frac{d^2 \varepsilon^3}{16 k_0 S^2 z^2 (1-\varepsilon)^2} \qquad (5)$$

$$z = 1 + \frac{25.4}{\pi d S N} \left(\frac{1}{2n} + \frac{(1+\beta)}{k} \right)$$

$$k = \frac{D_m}{d}$$

K_p : Permeability [m²]
ε : Porosity [-]
d : Wire diameter [m]
S : Shrinkage coefficient [-]
N : Mesh number [-]
n : Layer number [-]
D_m : Wick mean diameter [m]

effective thermal conductivity

$$\frac{1}{K} = \frac{1}{(1+\beta)}\left(\frac{1}{K'} + \frac{\beta}{k_l}\right) \quad ----(6)$$

$$K' = \frac{k_l \pi \sqrt{B^2 - A^2}}{A \log\left(\frac{B+\sqrt{B^2-A^2}}{B-\sqrt{B^2-A^2}}\right)}$$

$$A = \frac{k_l}{k_\omega - k_l}$$

$$B = \frac{\pi^2 d S}{8 P}$$

d : Wire diameter [m]
P : Pich [m]
S : Shrinkage coefficient [-]
k_l : Liquid phase thermal conductivity [W/m•K]
δ : Inter-layer clearance [m]
β : Inter-layer clearance ratio [-] ($\beta = \delta / 2d$)

Heat transfer resistance

$$R = \frac{\ln(d_o / d_i)}{2\pi k L} \quad ----------(7)$$

k : Thermal conductivity [W/m•K]
d_o : Diameter (out-side) [m]
d_i : Diameter (in-side) [m]
L : Length of heat transfer section [m]

Assume that these two parts are connected in parallel with respect to heat transfer.

(b) Assume that the surplus fluid cylindrically spreads over the inner surface of the screen wick and the connection of the heat transfer resistance are made in series.

The effective thermal conductivity of the wick was calculated by using equation (6) which takes account of inter-layer clearance β, while equation (7) was used to calculate the heat transfer resistances of fluid layer and container.

§VI. Comparison Between Culculation And Measurement

To validate the calculation, experiments were made by using a cupper-water heat pipe which length and inner diameter are 300 mm and 15 mm, respectively. The results of these experiments are shown in Figure 8, 9, 10. Figure 8 shows the relationship between heat flow and temperature difference. In Figure 8, dotted lines represent that calculla-tion made with the assumption of parallel connection of heat transfer resistances. Each lines corresponds to different values of inter-layer clearance. The calculation gave far small values than the measurement. The solid line repressents the calculation made with the assumption of series connection of heat transfer resistances. The experiments was repeated twice. The results of the first experiment are indicated by white circles while the second by black circless .

Obviously the calculation with the assumption of series connection of heat transfer resistances shows better agreement with the experiment.

Figure 9 shows the relationship between heat flow and temeprature difference between the evaporation and adiabatic zones. For lower values of heat flow, the agreement

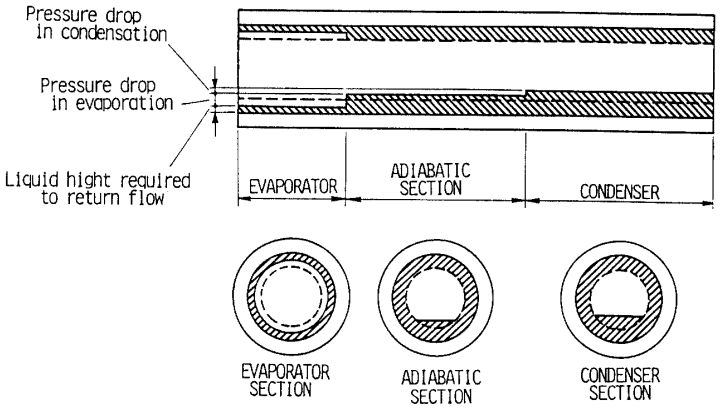

Fig. 6. The model distribution of working fluids.

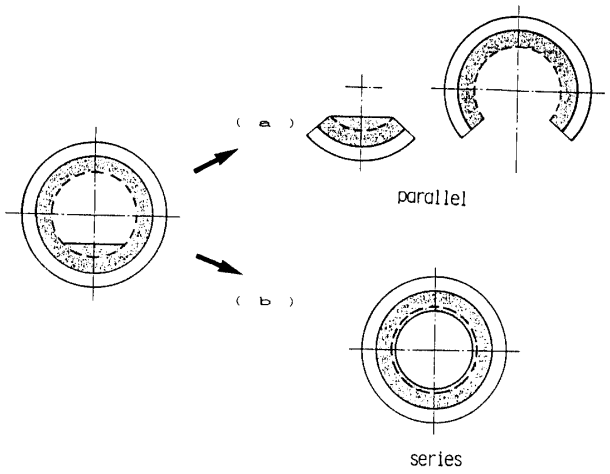

Fig. 7. Head transfer resistance model.

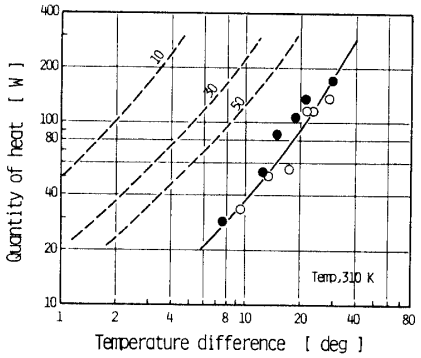

Fig. 8. The experimental results (evaporator-condenser).

between calculation and experiment is good, however, it is not for the higher values of heat flow. The calculated curve turns up because the fluid layer in the evaporation zone becomes thinner and heat resistance decreases as heat flow increases. If nucleate boiling occurs heat resistance should decrease more. Since the experimental curve shows that heat flow increases with almost the same gradient, something like vapor layer may have to be taken into consideration. However, the cause of disagreement is unknown.

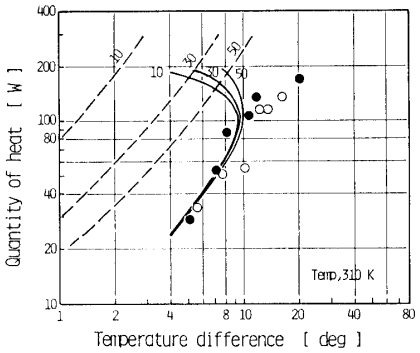

Fig. 9. The experimental results (evaporator-adiabatic section).

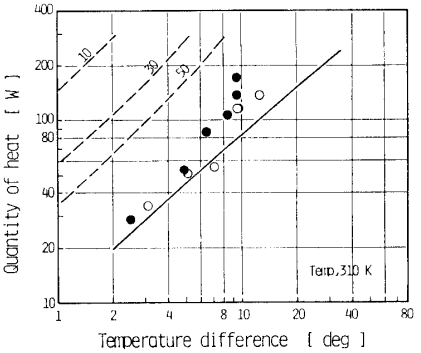

Fig. 10. The experimental results (condenser-adiabatic section).

Figure 10 shows the relationship bewtween heat flow and temperature difference between adiabatic and condensation zones. In this figure, the calculation gives higher heat resistance in higher heat flow region.

This is accounted for by the fact that fluid layer in the condensation zone becomes thicker as heat flow increases. However, with the assumption of the cylindrical layer of stagnant fluid in the adiabatic and condensation zones, we may have to impose a limit on the growth of stagnant fluid layer.

For futher investigation, a calculation was made with the assumption of series connection of heat transfer resistance. In this calculation, data of temperature shown in Figure 11 are used. These data have been presented in previous literature (2). Figure 12 shows the results of the calculation together with the measurement. In Figure 12, white circles represent the calculation while black circles the measurement. The accuracy of plotting the measurement is not very good because they were obtained from reading the drawn curve. In Figure 12, the top graph shows the total temperature difference, the middle the temperature difference between the evaporation and adiabatic zones, and the bottom the temperature difference between the adiabatic and condensation zones. Some corrections were made by ignoring such areas as the temperature is unreasonablly low due to uncondensed gas and by subtracting the quantity of fluid standing in such areas. With respect to the temperature difference between the evaporation and adiabatic zones good agreement was obtained between calculation and measurement.

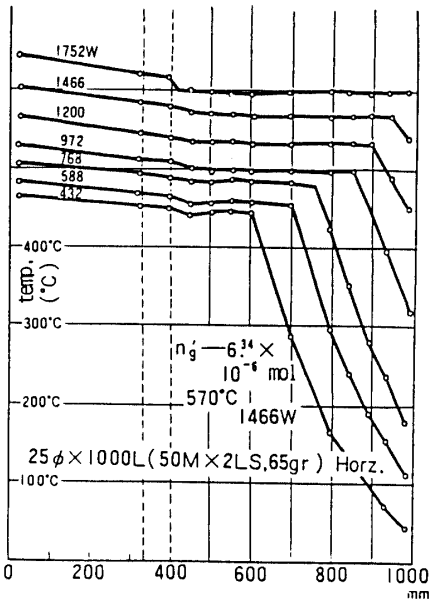

Fig. 11. Surface temperature profiles of sodium heat pipes (reference).

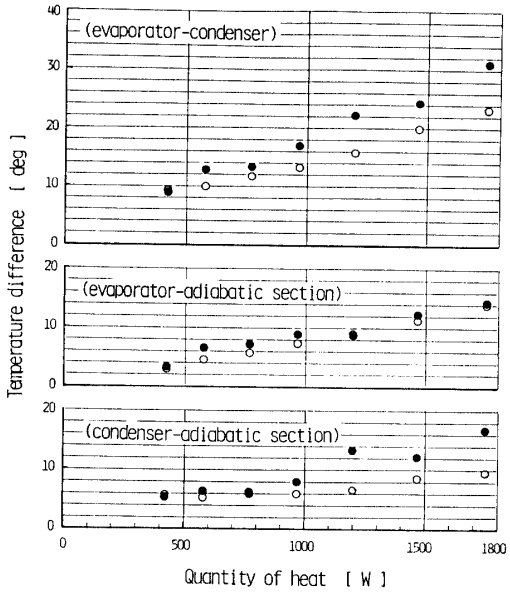

Fig. 12. Temperature difference to heat transfer quantity.

However, with respect to the temperature difference between the adiabatic and condensation zones, the measurement gave larger values of heat resistance which subsequently affect the accuracy of calculation for the total temperature difference.

§VII. Conclusion

(1) The heat flow and temperature distribution in a heat pipe containing the screen wick and being horizontally laid can be calculated with farely good accuracy by assuming that the depth of stagnant working fluid in the heat pipe varies step-wise as determined by the pressure losses in the evaporation and condensation zones, and that the standing fluid cylindrically adheres to the inner surface of the screen wick.

(2) In the evaporating zone, nucleating boiling seems to have small effect.

(3) More experimental research is necessary for further investigation.

References

[1] K. Oshima, *et al.*: Heat Pipe Engineering, Asakura pub (1979).
[2] I. Honda: High temperature Na-Hp, J. Metal Vol. 49–12, 1979.